Durability Assessment of 15- to 20-Year-Old GFRP Bars Extracted from Bridges in the US. II: GFRP Bar Assessment

Ali F. Al-Khafaji, S.M.ASCE[1]; Rudy T. Haluza, S.M.ASCE[2]; Vanessa Benzecry, S.M.ASCE[3]; John J. Myers, F.ASCE[4]; Charles E. Bakis, F.ASCE[5]; and Antonio Nanni, F.ASCE[6]

Abstract: A multilaboratory investigation into the durability of glass fiber–reinforced polymer (GFRP) bars extracted from eleven 15- to 20-year-old bridges in the US will be performed. Part 1 (Benzecry et al., forthcoming) of this two-paper series describes the bridges and presents data on the condition of their concrete, and Part 2 focuses on the condition of the bars. Constituent content, maximum water absorption, as-received moisture content, glass transition temperature (T_g), short bar shear (SBS) strength, and tensile strength will be evaluated. Scanning electron microscopy (SEM) and energy dispersive spectroscopy (EDS) will be performed. The fiber mass content of all bars was close to or greater than that specified in the current ASTM E1309 (ASTM 2011a) GFRP bar standard. SEM and EDS showed only slight signs of degradation, which was predominantly near the outer radius of the bars. The loss of SBS strength was slight to moderate in bars with control data for comparison. Tensile strength, which could only be evaluated in 1 bridge, showed a reduction of only 4.2% after 17 years of service. It was concluded that GFRP bars could be considered a promising replacement for steel reinforcement in bridge decks subjected to real-time field exposure. **DOI: 10.1061/(ASCE)CC.1943-5614.0001112**.

Author keywords: Glass fiber–reinforced polymer; Durability; Field performance; Strength; Physical properties.

Introduction

Corrosion-related damage in steel–reinforced concrete (RC) structures is expensive to repair and often requires expensive continuous monitoring (Nanni et al. 2014). There are >600,000 bridges in the US that have been built with steel RC and the estimated direct cost of repairs of these bridges is USD 8.3 billion (Koch et al. 2016). Glass fiber–reinforced polymer (GFRP) composite reinforcement bars have emerged as a potentially more durable replacement for steel in RC structures (ACI 2015). GFRP bars have many benefits, such as low cost-to-performance ratio, noncorrosive behavior, and high strength-to-weight ratio (ACI 2015).

The pore water solution of concrete is highly alkaline with a pH between 10.5 and 13.5 (Diamond 1981; Taylor 1987). Exposure to alkalis can deteriorate the tensile and longitudinal shear strength of GFRP bars (Nkurunziza et al. 2005). There are two major mechanisms for an alkali environment to damage fibers: (1) chemical attack on the glass fibers by alkalis, and (2) concentration of hydration products at the interface between the fibers and matrix (Mufti et al. 2007; Murphy et al. 1999). Although the resin matrix of composites gives a certain level of protection to the fibers from alkalis and moisture, migration of chemicals through the resin, void, or cracks to the fiber surface remains possible (Nkurunziza et al. 2005). Numerous aspects of GFRP structural behavior need to be examined, confirming that the long-term durability is potentially the most substantial barrier to increase its acceptance in the industry (Gooranorimi et al. 2017). Other barriers include concerns about brittleness and its initial cost compared with mild steel (Gooranorimi et al. 2017).

The performance of GFRP bars under laboratory-controlled aggressive environmental conditions (sometimes called accelerated testing) has been investigated by evaluating the tensile strength, tensile elastic modulus, short bar shear (SBS) strength, and bar or concrete bond strength following conditioning (Al-Salloum et al. 2013; Khatibmasjedi et al. 2020; Wang et al. 2017). In addition, the strength loss of GFRP bars is higher in alkaline solutions than in water (Al-Salloum et al. 2013). Kamal and Boulfiza (2011) investigated the effect of the simulated pore water solution of concrete on GFRP bars. Because the diffusion of moisture into the fiber–matrix interphase in a composite could cause fiber–matrix debonding and the presence of alkalis at the locations on the glass surface could lead to fiber degradation, researchers have investigated whether GFRP bars allowed both species to penetrate or allowed only water when blocking alkalis. The GFRP bars were immersed in five types of simulated concrete pore solutions, including sodium hydroxide (NaOH), potassium hydroxide (KOH), calcium hydroxide [$Ca(OH)_2$], NaOH + KOH, and NaOH + $Ca(OH)_2$, at elevated temperatures. X-ray mapping was used to assess alkali penetration. The results showed that fiber–matrix debonding

[1]Ph.D. Candidate, Dept. of Civil, Architectural and Environmental Engineering, Missouri Univ. of Science and Technology, 1401 N. Pine St., Rolla, MO 65409 (corresponding author). Email: aa7n6@mst.edu

[2]Ph.D. Candidate, Dept. of Engineering Science and Mechanics, Pennsylvania State Univ., 212 Earth-Engineering Science Building, University Park, PA 16802. ORCID: https://orcid.org/0000-0002-8455-9738. Email: rth5095@psu.edu

[3]Ph.D. Candidate, Dept. of Civil, Architectural and Environmental Engineering, Univ. of Miami, 1251 Memorial Dr., Coral Gables, FL 33146. Email: v.benzecry@umiami.edu

[4]Professor, Dept. of Civil, Architectural and Environmental Engineering, Missouri Univ. of Science and Technology, 1401 N. Pine St., Rolla, MO 65409. Email: jmyers@mst.edu

[5]Distinguished Professor, Dept. of Engineering Science and Mechanics, Pennsylvania State Univ., 212 Earth-Engineering Science Building, University Park, PA 16802. ORCID: https://orcid.org/0000-0002-6834-5318. Email: cbakis@psu.edu

[6]Professor & Chair, Dept. of Civil, Architectural and Environmental Engineering, Univ. of Miami, 1251 Memorial Dr., Coral Gables, FL 33146. ORCID: https://orcid.org/0000-0003-2678-9268. Email: nanni@miami.edu

Note. This manuscript was submitted on June 16, 2020; approved on November 12, 2020; published online on January 23, 2021. Discussion period open until June 23, 2021; separate discussions must be submitted for individual papers. This paper is part of the ***Journal of Composites for Construction***, © ASCE, ISSN 1090-0268.

occurs in some specimens. However, the glass fibers and matrix remained intact and there was no penetration of alkalis into the matrix. The debonding, which occurred only in specimens subjected to 75°C, was believed to be due to the hydrolysis of fiber sizing at high temperature.

In addition, research has been performed to create accelerated aging procedures and predictive models for the long-term strength of GFRP bars in concrete. Different models have been developed for accelerated aging tests of GFRP bars, such as the diffusion model (Saadatmanesh and Tannous 1999) and the Arrhenius model (Porter and Barnes 1998; Chen et al. 2006). In general, these models suggested that higher temperatures, higher alkaline ion concentrations, and longer times are more detrimental to strength. Material constants used in these models depend on the exact constituents of the bar, such as the type of glass in the fiber, type of coupling agent on the fiber, type of resin, and type of filler in the resin (Khatibmasjedi et al. 2020). In addition, the degree of access of the aggressive agents into the bar, for example, through concrete cracks, has a notable influence on the rate of bar degradation (Yang et al. 2016).

Limited research has been conducted into field exposure cases. Bakis et al. (2005) showed that strength loss in GFRP bars extracted from loaded concrete beams stored in natural (nonaccelerated) indoor and outdoor environments for ≤ 3 years was negligible. Trejo et al. (2011) observed 12%–26% strength loss in GFRP bars extracted from unloaded concrete specimen stored in an outdoor environment for 7 years. Benmokrane et al. (2018) investigated the physicochemical attributes of GFRP bars extracted from bridge barrier walls after 11 years of service and found no changes. Additional information on the durability of GFRP bars following field service needs to be collected to improve the understanding of the long-term service potential of GFRP bars in realistic situations and to assist the development of appropriate strength retention factors for design purposes (Micelli and Nanni 2004).

In the investigation described in this paper, mechanical and physicochemical tests are carried out on GFRP bars extracted from 11 existing bridges located in various US states to assess the condition and strength of the bars after 15–20 years of service. The types of tests performed include fiber content, water absorption, moisture content, scanning electron microscopy (SEM), energy dispersive spectroscopy (EDS), glass transition temperature (T_g), SBS (SBS) strength, tensile strength, and constituent volume contents by image analysis. These tests are performed to improve the durability database for GFRP bars subjected to long-term service conditions. Investigations of this type have been identified as high priority in a recent workshop sponsored by the US DOT and address a critical need to document and disseminate information that overcomes barriers for the wider adoption of fiber–reinforced polymer (FRP) composites in infrastructure (Sheridan et al. 2017).

Bar Testing Program

In the first part of this two-paper series (Benzecry et al., forthcoming), information on the bridges from which the bars were extracted, bar extraction methods, and the specimen labeling scheme are detailed. Fig. 1 shows photographs of the bars from all the bridges investigated in this research. The list of states in which the bridges are located is given in the first column of Table 1. Before testing, the bars were brushed and gently scraped to remove obvious contaminants, such as residual cementitious paste.

Fiber Mass Content

A burn-off procedure based on ASTM D2584 (ASTM 2011c) was implemented to evaluate fiber mass content. Bar specimens weighed approximately 5 g (0.011 lb). The burn-off temperature of 575°C (1,067°F) eliminated the matrix material but not the sand particles and helical fiber wrap on some of the bars, the filler particles in the matrix, and the fibers. The sand particles and helical wrap were excluded from the mass of the longitudinal fibers and residual filler that remained after burn-off. Following the fiber mass fraction calculation method in the ASTM D7957 (ASTM 2017a) GFRP bar specification, the mass fraction of fiber was determined by dividing the mass of the fibers and residual filler divided by the mass of these same materials plus the mass of the burned-off resin.

Water Absorption

Water absorption to equilibrium in 50°C (122°F) distilled water was measured using ASTM D570 (ASTM 2017b). Specimens of approximately 25 mm (1.0 in.) length were preconditioned in an oven at 40°C (104°F) for 48 h to minimize variances in near-surface moisture that could have accrued due to storage in different laboratory environments before absorption testing. Using the preconditioned weight as the reference weight, the weight gain and time to equilibrium weight were then obtained by repeated measurements until the increase in weight per 2-week period, as shown by three consecutive weighings, averaged <1% of the total increase in weight or 5 mg (0.0002 oz) whichever was more. The 5 mg (0.0002 oz) criterion was controlled in these experiments.

Moisture Content

The moisture content of the as-received (without preconditioning) bars was measured by drying 13 mm (0.5 in.) specimens to equilibrium in a forced-air oven set to 80°C (176°F), as described in Procedure D of ASTM D5229 (ASTM 2010). During testing, specimens were weighted every day for 10 days and every week thereafter. The dry-out test was terminated when the weight changes of all of the specimens were <0.02% for two consecutive 7-day periods and examination of the moisture content versus square root of time plot supported the percent change criteria that effective equilibrium had been reached. No preconditioning was conducted on the moisture content specimens. Data from the moisture content tests reflect field exposure as well as laboratory exposure after extraction.

SEM

SEM on the polished cross sections of bars was performed to visually identify signs of microstructural degradation, such as cracks in the fibers and matrix, voids, and fiber–matrix debonding. The inspected surfaces were sanded with 1,200 grit abrasive paper, polished with a 0.2 μm (US units) abrasive paste, and then plated with gold.

EDS

EDS was used to evaluate the chemical composition of the surface of the SEM specimens. Because wet concrete is highly alkaline, the potential for degradation of the fibers and matrix due to excessive amounts of sodium (Na), potassium (K), and calcium (Ca) that penetrated the bar must be investigated (Mufti et al. 2007). Moreover,

Fig. 1. Bars from the 11 bridges.

if the fibers were shown to contain zirconium (Zr), then it was concluded that the bars were alkali-resistant glass rather than traditional E-glass (Nkurunziza et al. 2005). EDS can detect elements Na, K, and Ca. A 10–20 kV electron beam was used for the EDS testing. The size of the region of evaluation was approximately ≤1 μm (US units), which allowed for the separate evaluation of fibers and matrix (but not necessarily resin and filler).

The T_g

The T_g can be defined as the temperature range where the polymer substrate changes from a solid glassy material to a rubbery material (Becker and Locascio 2002). In this paper, differential scanning calorimetry (DSC) according to ASTM E1356 (ASTM 2014a) was used to characterize the T_g of bars from 10 of the 11 bridges and dynamic mechanical analysis according to ASTM E1640 (ASTM 2013) was used for 1 bridge. For DSC testing, small pieces of material that weighed 10–15 mg were cut from a bar and preconditioned in an oven for 48 h at 48°C (118°F) to remove surface moisture. During the DSC test, the temperature was ramped upward once at 5–10°C/min (41–50°F/min). The midpoint method was used to determine the T_g.

Table 1. Average fiber mass content for each bridge

Bridge (state)	Number of specimens	Fiber mass content (%)	Std. deviation (%)
Gill's Creek (VA)	6	72.1	1.78
O'Fallon Park (CO)	6	72.9	1.93
Salem Ave. (OH)	3	72.5	0.06
Bettendorf (IA)	3	73.3	1.29
Cuyahoga County (OH)	15	76.4	2.41
McKinleyville (WV)	6	73.5	2.82
Thayer Road (IN)	3	76.5	0.078
Roger's Creek (KY)	5	69.2	1.08
Sierrita de la Cruz Creek (TX)	9	76.4	—
Walker Box Culvert (MO)	4	82.8	—
Southview (MO)	4	73.4	—

SBS

SBS tests to evaluate the longitudinal shear strength of the bars were carried out following ASTM D4475 (ASTM 2016). The span to depth ratio was from 3 to 6 based on the specimen length. The loading rate was 1.27 mm/min (0.05 in./min). Due to the limited number of bars of suitable length taken from the 102 mm diameter (4 in.) concrete cores, a minimum of 3 test repetitions per bridge could not be achieved for all the bridges and only 8 bridges could be tested for shear strength.

Tensile Test

Although the longest witness bars from the Sierrita de la Cruz Creek Bridge in Amarillo, Texas, were too short to test according to ASTM D7205 (ASTM 2011b), they were of sufficient length to evaluate using a modified tensile test method developed in this investigation. The modified tensile strength test method entailed slicing a bar longitudinally into flat coupons that could be tested with short lengths using ASTM D3039 (ASTM 2014b). The three 16 mm diameter (0.63 in.) witness bars extracted from the Sierrita de la Cruz Creek Bridge were cut into nine thin rectangular coupons utilizing a computer numerical control wet saw with a diamond abrasive blade, as shown in Fig. 2(a). The 3 × 11 × 254 mm (0.11 × 0.43 × 10 in.) (thickness × width × length) coupons were fitted with 57 mm (2.24 in.) composite tabs, resulting in a gauge length of approximately 140 mm (5.5 in.).

Pristine current production bars similar in shape, size (16 mm diameter), and manufacturer to the bars extracted from the Sierrita de la Cruz Creek Bridge were obtained and tested as is (ASTM D7205, ASTM 2011b) and as flat coupons. The specific fiber and matrix

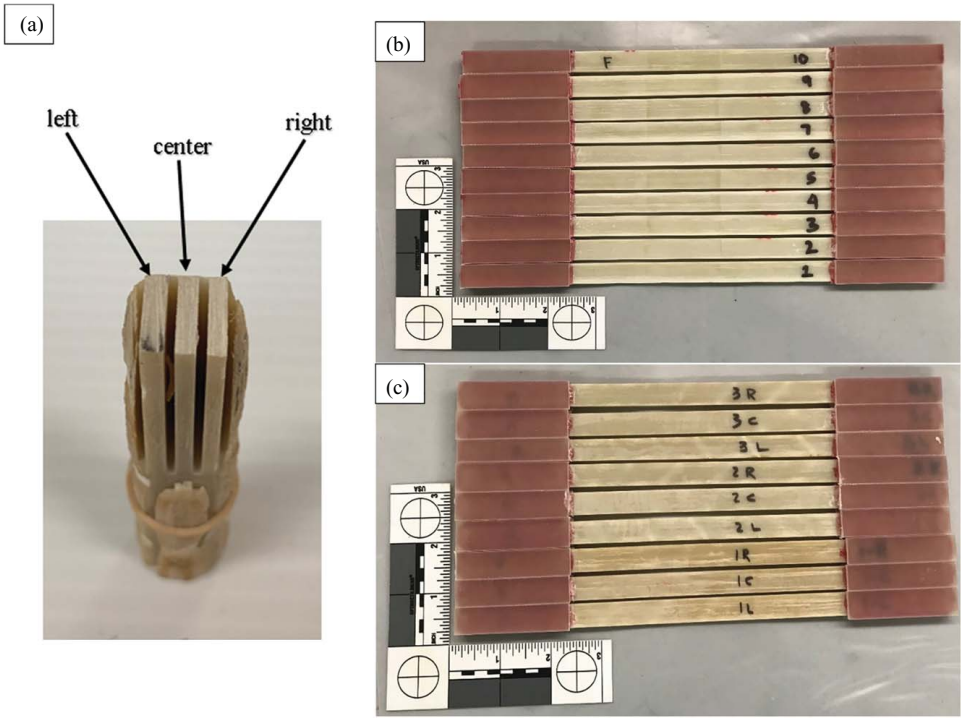

Fig. 2. Showing: (a) method to cut flat coupons for tensile testing; (b) current production tensile coupon; and (c) extracted tensile coupons.

materials in the current production bars differed from those used in the bars installed in the bridge in 2000. The tests from current production bars enabled the calculation of a ratio of full-bar strength to flat coupon strength. This ratio, which was assumed to apply to the environmentally exposed bars from 2000 as well, was then used to estimate the full-bar strength of the extracted bars based on their measured coupon strength. Finally, the estimated full-bar strength of the extracted bars is compared to published strength data for pristine 16-mm (0.63 in.) bars installed in the bridge in 2000.

Photographs of the extracted and current production coupons with tabs are shown in Figs. 2(b and c). All coupons were tested using a 100 kN (22.5 kips) servo hydraulic load frame and a 50 mm (2.0 in.) extensometer to measure strain. The full-size bars were tested in an 890 kN (200 kips) Baldwin screw–driven universal test frame and a 100 mm (4.0 in.) extensometer was used to record strain. Both tests were performed at a rate of 2 mm/min (0.08 in./min.). Young's modulus of the coupons and bars was measured by the chord method between strains of 1,000 and 3,000 $\mu\epsilon$.

Constituent Volume Contents by Image Analysis

Fiber, matrix, and void volume contents were measured by analyzing area fractions in polished transverse cross sections of the bars. The test was based on the assumption that all features observed on a transverse cross section extended throughout the entire length of the bar (Little et al. 2012). To minimize section bias in computing void volume fractions (Ghiorse 1991; Little et al. 2012), statistics on the constituent volume contents were obtained based on the analysis of 30 individual micrographs for each bar. The micrographs were obtained at evenly spaced intervals along a radial path that emanated from the center of the bar for fiber content and along the full diameter for void content. Due to the similarity in the brightness of the glass fibers and the polymer section of the matrix, a MATLAB script was employed to collect manually-selected fiber–matrix boundaries and to use these boundaries to automatically calculate fiber area in a given micrograph. The fibers were assumed to be circular in cross section, and three observable points were selected on the circumference of the fiber–matrix boundary, which defined each fiber in the micrograph. Initial attempts that involved thresholding and shape detection techniques were unsuccessful; the boundary between the fiber and matrix was easily identifiable as a thin, relatively dark circle for the vast majority of fibers. The relatively low brightness of the voids allowed the void area to be calculated based on the proportion of image pixels that were darker than a carefully selected threshold. The matrix volume content, which consisted of polymer and filler, was determined by subtraction of the fiber and void volume percentages from 100%. Due to the time-intensive nature of this image analysis approach, only three bars from the O'Fallon Bridge (West of Denver, CO) were analyzed for constituent volume content.

GFRP Test Results and Discussion

Fiber Mass Content

Table 1 gives the fiber mass contents for bars from each bridge. In all bridges except for one, the fiber mass content, which included resin filler particles but excluded larger sand particles and helical fiber wraps added to some bars for bond enhancement, exceeded 70% [the current requirement for GFRP bars that satisfy ASTM D7957 (ASTM 2017a)]. Bars from Roger's Creek Bridge (Bourbon County, Kentucky) had fiber mass content only fractionally less than the current standard of 69.2%.

Fig. 3. Part of the helical wrap fell off one bar from the Cuyahoga Bridge during 50°C water absorption testing.

Water Absorption

Water absorption at 50°C (122 F) was evaluated on bars from 8 of the 11 bridges. Several observations were noted that could affect the weight of the bar specimens. A loss in helical wrap was noted when the Cuyahoga Bridge (Southeastern lake, Erie Snowbelt, Ohio) specimens were soaked in water, as shown in Fig. 3. For continuity in the data, the weights of these large pieces of material were recorded along with the remainder of the specimens. Smaller particles on the surface of the bars, such as sand and residual cementitious material, were observed to fall off during conditioning, but the mass of these particles could not be tracked.

Fig. 4 shows the weight change at equilibrium versus time to reach equilibrium for each specimen. The current ASTM GFRP bar specification [ASTM D7957 (ASTM 2017a)] stipulates a qualification limit of 1% water absorption in pristine bars as an indication of bar durability. Bars from five of the eight bridges had equilibrium water absorption values of <1%, with the exceptions being those from Gills Creek Bridge (1.5%), Bettendorf Bridge (Bettendorf, Iowa) (2.1%), and Cuyahoga Bridge (Franklin County, Virginia) (1.5%). The times to equilibrium in the latter three bridges were considerably >150 days, and the others were approximately 80 days.

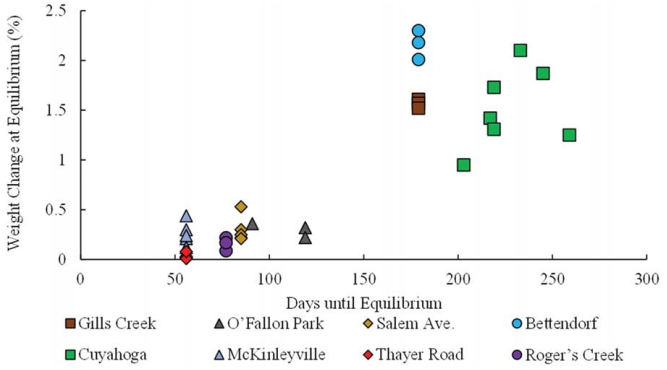

Fig. 4. Equilibrium weight change and time to reach equilibrium for bars immersed in 50°C water.

Table 2. Results of the 50°C water uptake tests

Bridge	Number of specimens	Avg. 24-h weight change (%)	Avg. weight change at equilibrium (%)	Avg. days until equilibrium
Gill's Creek	3	0.58	1.57	179
O'Fallon Park	3	0.01	0.30	110
Salem Ave.	5	0.10	0.30	85
Bettendorf	3	0.54	2.16	179
Cuyahoga	7	0.28[a]	1.52	228
McKinleyville	6	0.10	0.23	56
Thayer Road	5	0.02	0.02	56
Roger's Creek	3	0.05	0.16	77

[a]This average reflects only five specimens because two of the specimens showed erroneous results for this measurement.

Table 2 gives the average weight change measured at 24 h and at equilibrium as well as the average time required to reach equilibrium for each bridge. It is emphasized that the water uptake measurements are relative to the existing water content of the bars following the superficial 48 h, 40°C (104°F) preconditioning regimen. For O'Fallon and Cuyahoga bars, the water content at the beginning of the uptake test (i.e., after preconditioning) was approximately 0.36%, according to dry-out tests performed at 80°C using ASTM D5229 (ASTM 2010). Therefore, the actual moisture content in the bars at equilibrium could be expected to be approximately 0.36% more than the values listed in Table 2. Some of the extracted bars could exceed the 1% absorption limit of ASTM D7957-2017 (ASTM 2017a); it is noted that the bars evaluated in this paper were manufactured before the existence of contemporary standards. In addition, as shown in the following section, the water content of the bars after 15–20 years of service was well below 1%.

Moisture Content

As-received (without preconditioning) moisture content was evaluated by drying out bars from two bridges, O'Fallon Park and Cuyahoga, at 80°C (176°F) (Table 3). Fig. 5 shows the weight change at equilibrium versus the time required for individual specimens to reach equilibrium. All of the specimens reached equilibrium after 49 days. Weight loss was observed to be nonmonotonic, potentially due to the variations in the humidity level in the laboratory. The O'Fallon Bridge bars had less as-received moisture (0.32% on average) than the Cuyahoga Bridge bars (0.44% on average). For reference, both of these values were significantly <1% equilibrium value allowed by ASTM D7957 for 50°C (176°F) water immersion, although the bars were not necessarily expected to be saturated to such a high degree by field conditioning.

Table 3. Results of 80°C dry-out tests

Bridge	Number of specimens	Avg. 24-h weight change (%)	Weight change at equilibrium (%)	Avg. days until equilibrium
O'Fallon Park	3	−0.150	−0.320	40
Cuyahoga	5	−0.218	−0.436	34

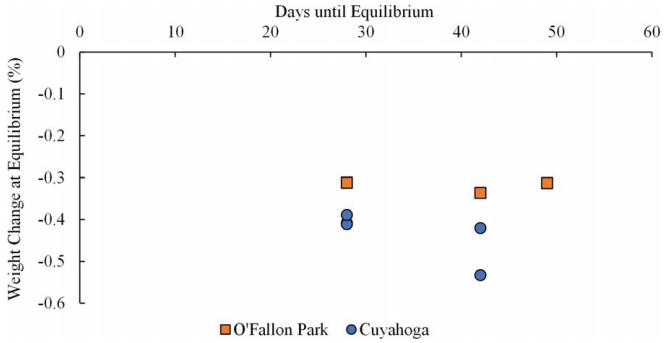

Fig. 5. As-received moisture content of bars determined by drying at 80°C, along with time required to reach equilibrium.

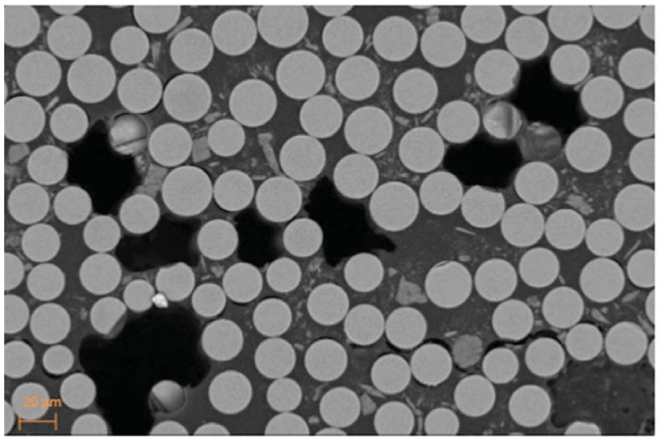

Fig. 6. SEM image of Gill's Creek Bridge.

SEM

SEM was performed on bars from all 11 bridges. In general, minimal evidence of environmental damage to the fibers, matrix, or fiber–matrix interface was seen. For example, in Gill's Creek Bridge, a few matrix and interfacial cracks were seen near voids that were located near the outer radius of the bar. Moreover, the number of fibers that showed signs of environmental degradation was approximately 192 out of 352,000 fibers (0.05%), estimated by counting fibers with and without signs of environmental damage in one quadrant and then multiplying by four. Fig. 6 shows an SEM image of a bar from Gill's Creek Bridge. In addition, the Cuyahoga Bridge bars displayed a small percentage of environmentally damaged fibers (Fig. 7). In these quantitative analyses of environmental damage in the fibers, damage attributed to specimen preparation, such as chipped or cracked fibers that had weak matrix support (e.g., located near a void), was omitted from consideration.

In the bars from Roger's Creek and McKinleyville Bridges, the incidence of environmentally damaged fibers, matrix, and interfaces was similar to or less than that seen in the Cuyahoga and

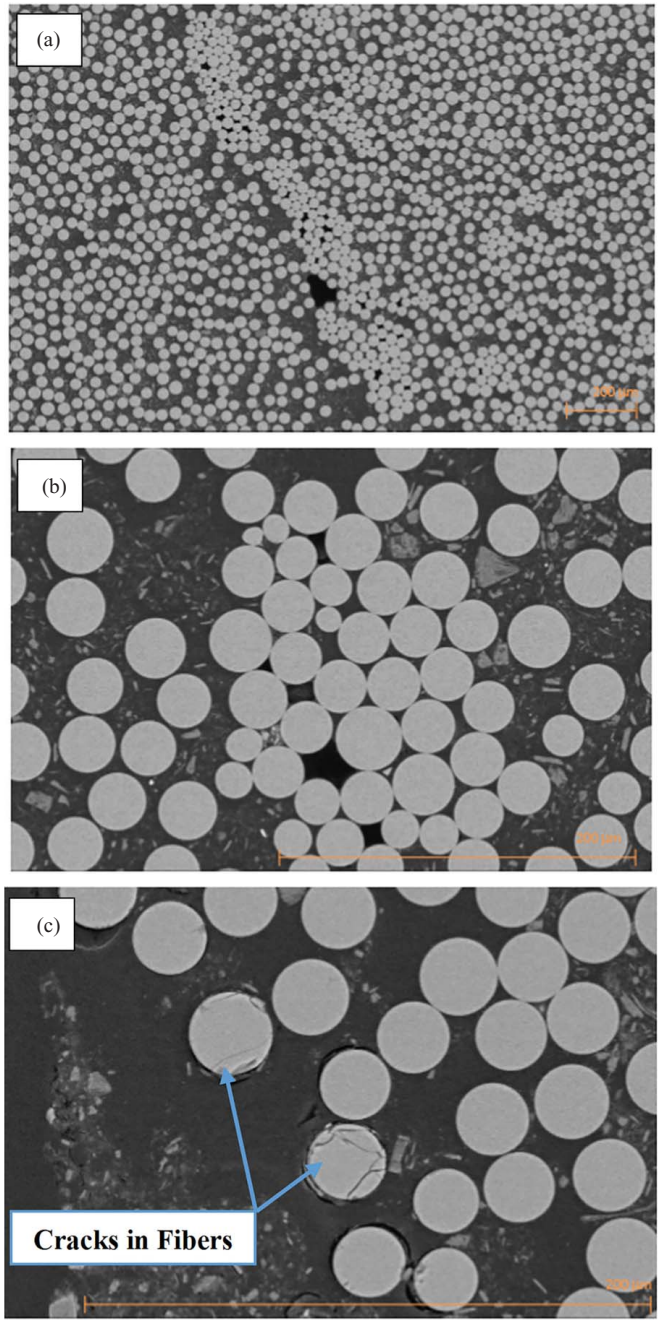

Fig. 7. SEM images of a bar from the Cuyahoga Bridge: (a) ×100 magnification; (b) ×700 magnification; and (c) ×1,000 magnification.

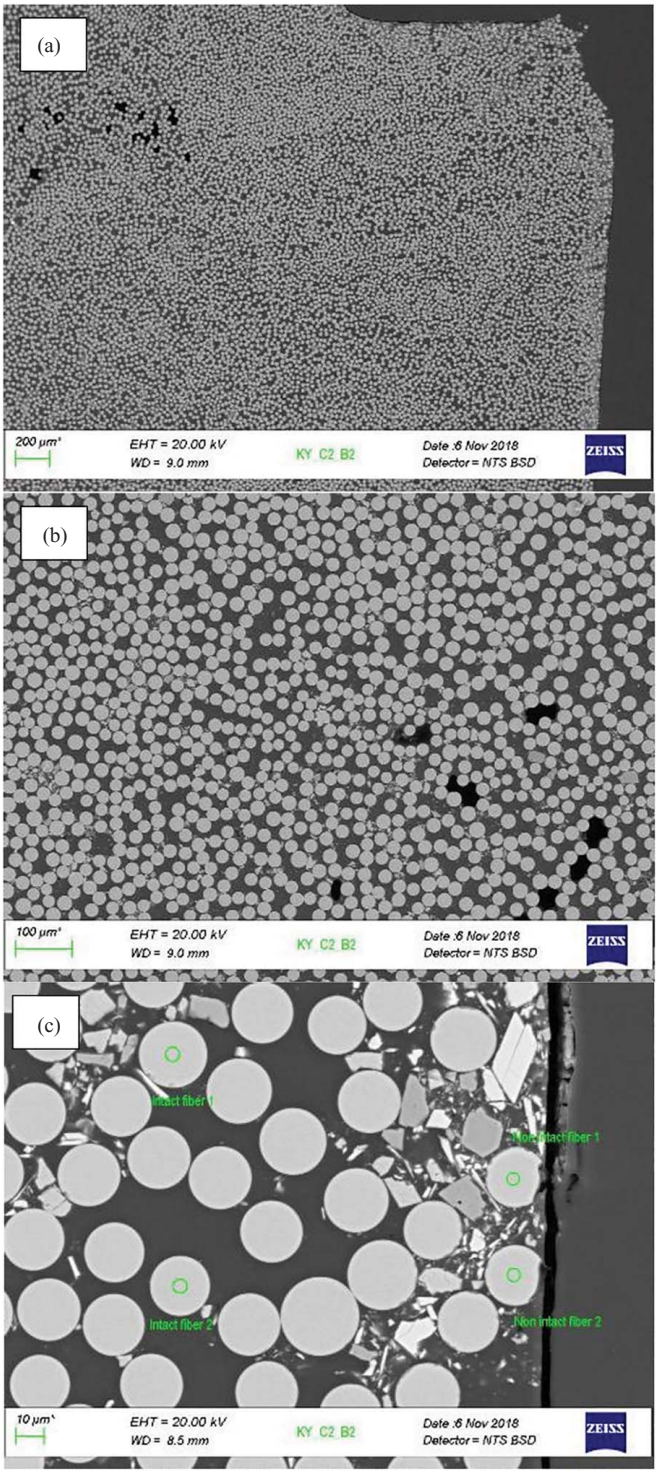

Fig. 8. SEM images of a bar from the Roger's Creek Bridge: (a) ×50 magnification; (b) ×100 magnification; and (c) ×800 magnification.

Gills Creek bars. Fig. 8 shows representative SEM images from Roger's Creek Bridge. Damage attributed to environmental effects was confined to regions near the outer radius of the bar.

In the Thayer Road Bridge, fiber damage was found in some bars, but was believed to be caused by the particular manufacturing procedure used to make the bars. The interior region of the bar showed negligible fiber damage; numerous fibers at the outside radius appeared to be partially removed as if they were abraded during manufacture (Fig. 9).

EDS

Bars from all bridges were evaluated by EDS. The EDS results are presented as histograms of counts detected versus the energy level of the X-rays emitted by the surface, where the energy level depends on the element that emits the X-rays. In all bars, there were no signs of Zr, which confirmed that the fibers used to make the bars were not alkaline-resistant fibers (Kamal and Boulfiza 2011). Magnesium (Mg) was found in some bars, which indicated conventional E-glass and those without Mg indicate acid-resistant (ECR) E-glass. In the fiber regions of all bars, the main elements were silicon (Si), aluminum (Al), and Ca. Some of the bars showed Na in their analysis. Reference bars without environmental exposure

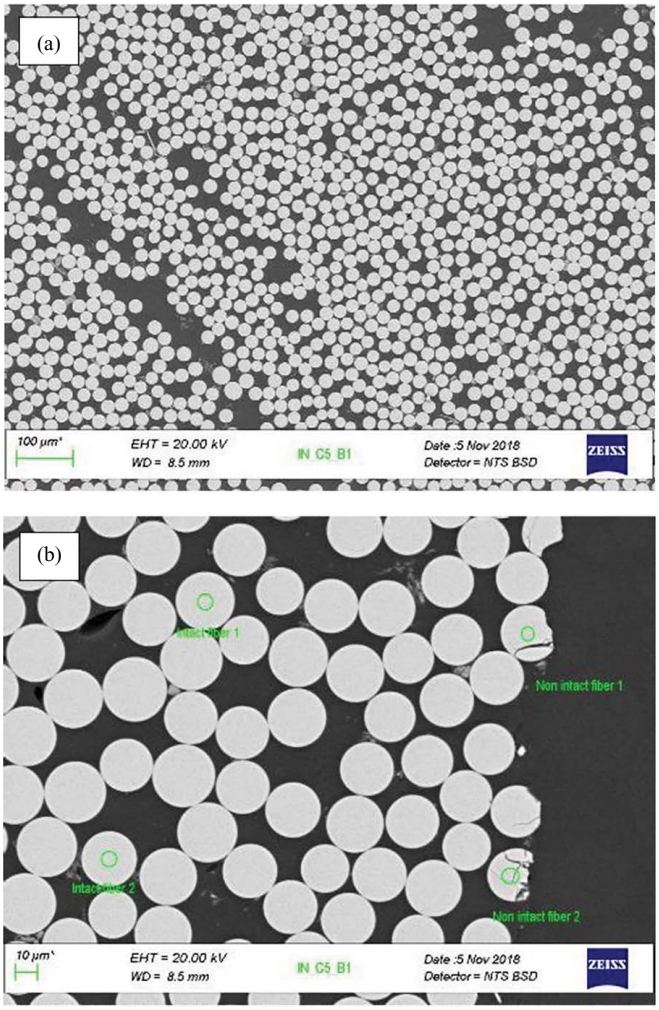

Fig. 9. SEM images of a bar from the Thayer Road Bridge: (a) × 100 magnification; and (b) × 800 magnification.

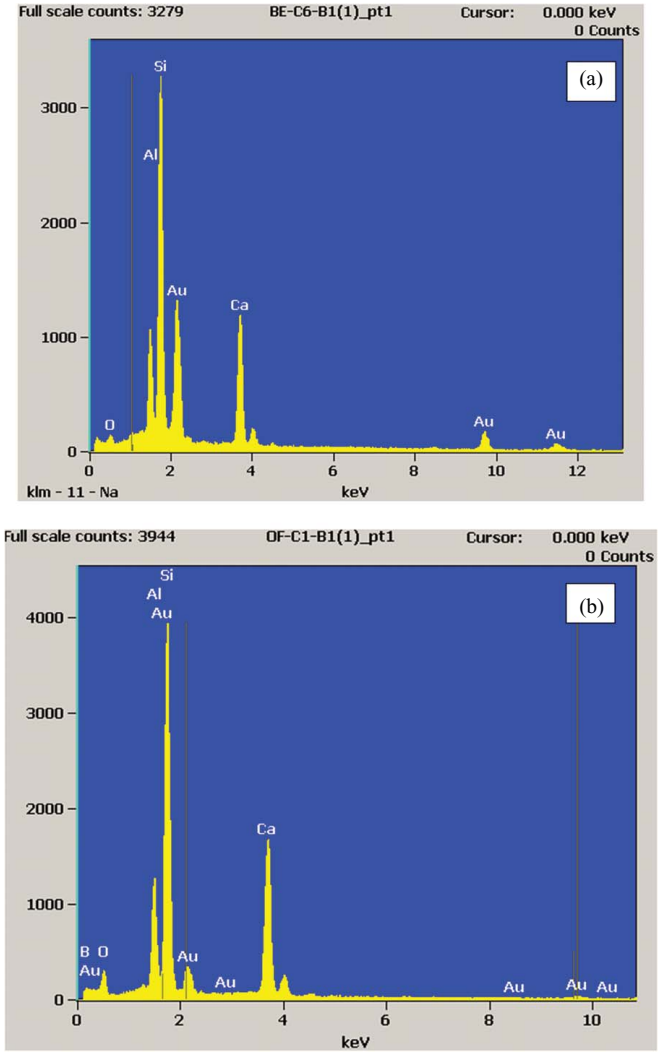

Fig. 10. EDS test results for bars from: (a) Bettendorf Bridge; and (b) O'Fallon Bridge.

would be required to discern changes in Na over time. The presence of gold (Au) in the EDS results was simply an artifact of the gold coating used to make the specimens electrically conductive for SEM. For the resin, the main element, carbon (C), was found in abundance.

Representative EDS results for the Bettendorf and O'Fallon bars (Fig. 10) did not show evidence of environmental attack, which would be manifested as Na, K, and Ca present in the resin. However, for the Southview Bridge (Fig. 11), Na was found in the resin, but not in the fiber. Na in the resin indicated that the GFRP bar was under environmental attack, especially considering that the concrete tests showed a high pH and no signs of carbonation (Benzecry et al., forthcoming). In addition, the lack of Na in the fiber confirmed that the Na in the resin came from the environment rather than the fiber.

In the bar extracted from the Sierrita de la Cruz Creek Bridge, Na was found in the resin as well as the fiber [Fig. 12(a)]. In addition, EDS was carried out on pristine new generation bars that were similar to the bars extracted from the Sierrita de la Cruz Creek Bridge [Fig. 12(b)]. The Na emittances were similar in both tests, which provided no evidence of chemical attack (leaching, alkali hydrolysis, or both) of the fibers in the bars of the Sierrita de la Cruz Creek Bridge.

Glass Transition Temperature

Extracted bars from all bridges had T_g values between 80°C (176°F) and 115°C (239°F), as given in Table 4. For reference, ASTM D7957 (ASTM 2017a) requires a T_g of ≥100°C. Therefore, bars from several bridges showed T_g values less than the ASTM D7957 lower limit. Without T_g data from bars that were produced approximately 20 years ago, the reason for low T_g values in some bars could only be conjectured in this paper. For example, certain types of bar could have been made with a low T_g resin system, before contemporary standards were developed. In addition, incomplete curing would be manifested by a T_g less than the potential that is inherent in polymer chemistry.

SBS

Table 5 lists the apparent shear strengths and nominal diameters of the bars tested, along with the strengths of control bars and dowel bars. The control bars refer to pristine bars that were tested when the bridges were built (Gooranorimi and Nanni 2017). Only the Cuyahoga and Sierrita de la Cruz Creek Bridges have control bars. Dowel bars refer to smooth, round E-glass–vinyl ester rods that are currently manufactured by the same manufacturer that made the

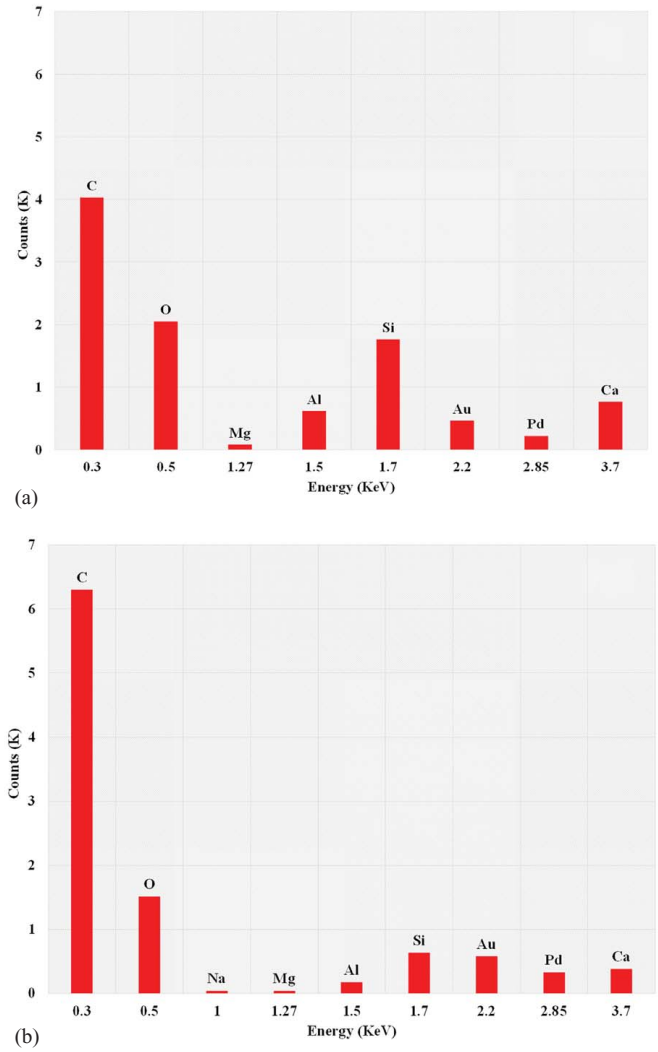

Fig. 11. EDS test results for a bar from Southview Bridge of: (a) fiber; and (b) resin.

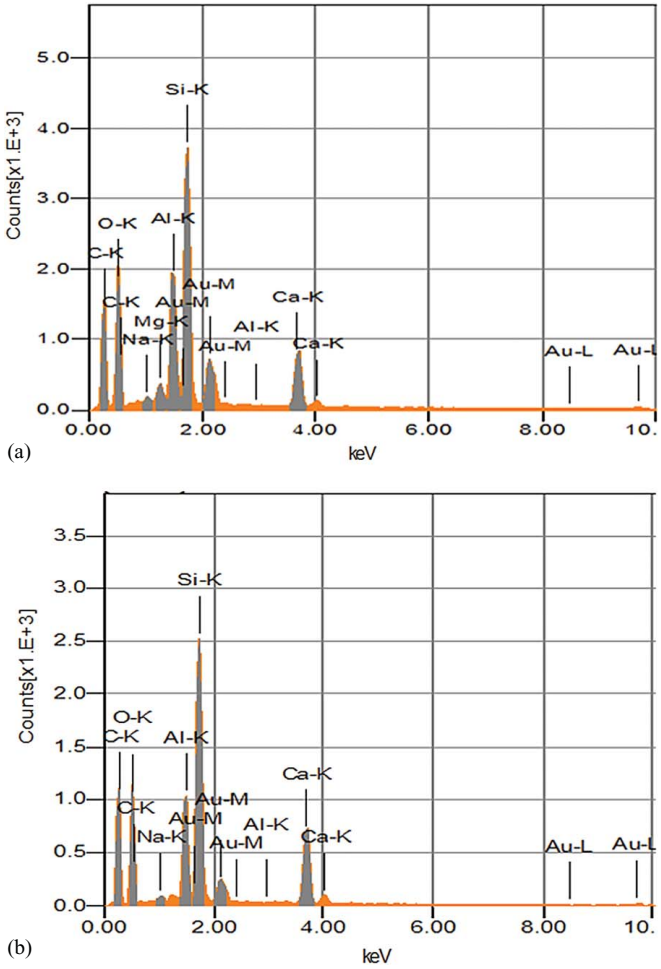

Fig. 12. EDS test results for bars from the Sierrita de la Cruz Creek Bridge: (a) extracted bars; and (b) pristine new generation bars.

bars in the bridges listed in Table 5 (Owens Corning 2018). In addition, the dowel bars have the same diameter as the bars in the bridges. Dowel bar strengths were provided as a rough measure for comparison with SBS strengths, in particular, for bridges that lacked control bars.

The SBS strength of the extracted bars was from 30 MPa (4,316 psi) to 47 MPa (6,809 psi). For the three bridges with control bars, it was seen that the extracted bars retained between 72% and 92% of their initial strength. The Cuyahoga and Sierrita de la Cruz Creek (19 mm) bars, which were at the lower end of the strength retention spectrum (72% and 76%, respectively), were noted to have uniquely low span-to-diameter ratios in relation to the 3–6 range recommended in ASTM D4475 (ASTM 2016), which might have contributed to their relatively low strengths. Multiple specimens, ideally of greater span-to-diameter ratio, are required to confirm this hypothesis.

For the dowel bar strengths, three of the extracted bars (O'Fallon Park, Cuyahoga, and Sierrita de la Cruz Creek that were 19 mm) were significantly (20%–40%) weaker and the remainder were within approximately ±10%. It is noted that the O'Fallon Park and Cuyahoga bars had the two lowest T_g values, which together with low shear strengths could be consistent with improper curing or chemical degradation of the resin that could not be detected by the other test methods.

Table 4. Average T_g results for all bars

Bridge	Average T_g [°C (°F)]
Bettendorf	109 (228)
Cuyahoga	92 (198)
Gill's Creek	95 (202)
O'Fallon Park	80 (176)
Salem Ave.	108 (226)
Roger's Creek	95 (203)
Sierrita de la Cruz Creek[a]	115 (239)
Walker Box Culvert[a]	112 (233)
Southview[a]	101 (213)
McKinleyville[b]	95 (202)
Thayer Road[b]	87 (189)

[a]T_g obtained with dynamic mechanical analysis rather than DSC.
[b]The lower of two transition temperature is reported.

Tensile Test

The tensile test results for flat coupons cut from Sierrita de la Cruz Creek Bridge 16 mm witness bars indicated an ultimate strength of 622 MPa (90.2 ksi) and an elastic modulus of 47.1 GPa (6,931 ksi), as given in Table 6. The stress–strain curves for the extracted coupons were approximately linear (Fig. 13), as commonly seen in a test of a typical full-size GFRP bar. Tables 7 and 8 list the strength and moduli of current production 16 mm bars tested as flat coupons and full bars, respectively. To calculate the correlation factor

Table 5. Average apparent shear strength from short beam shear tests

Bridge	Nominal diameter [mm (in.)]	Extracted bar strength [MPa (psi)]	Control bar strength [MPa (psi)]	Dowel strength [MPa (psi)][a]
O'Fallon Park	22 (0.88)	42 (6,115)	—	53 (7,687)
Salem Ave.	19 (0.75)	45 (6,459)	—	47 (6,800)
Cuyahoga	19 (0.75)	30 (4,316)	41[b] (5,956)	47 (6,800)
McKinleyville	10 (0.38)	36 (5,214)	—	36 (5,220)
Thayer Road	16 (0.63)	47 (6,809)	—	42 (6,092)
Sierrita de la Cruz Creek	16 (0.63)	42 (6,047)	45[c] (6,540)	42 (6,092)
Sierrita de la Cruz Creek	19 (0.75)	37 (5,361)	49[c] (7,040)	47 (6,800)
Southview	19 (0.75)	44 (6,340)	—	47 (6,800)
Southview	13 (0.50)	38 (5,558)	—	38 (5,511)
Walker	6.4 (0.25)	33 (4,828)	—	35 (5,000)

[a]Dowel bars currently produced by same manufacturer that made the bars installed in the bridges (Owens Corning 2018).
[b]Measured by bar manufacturer in 2000.
[c]Measured by bar manufacturer in 2000, as reported in Gooranorimi et al. (2017).

Table 6. Tensile test results for flat coupons extracted from the 16-mm bars in the Sierrita de la Cruz Creek Bridge

Specimen ID	Ultimate strength [MPa (ksi)]	Elastic modulus [GPa (ksi)]
1L	—	—
2L	625 (90.7)	47.8 (6,926)
3L	513 (74.4)	—
1R	660 (95.7)	—
2R	601 (87.1)	49.7 (7,214)
3R	560 (81.2)	44.7 (6,489)
1C	642 (93.1)	44.8 (6,498)
2C	691(100.2)	48.5 (7,036)
3C	686 (99.4)	—
Average	622 (90.2)	47.1 (6,831)
Std. deviation	62 (9.0)	2.2 (319)

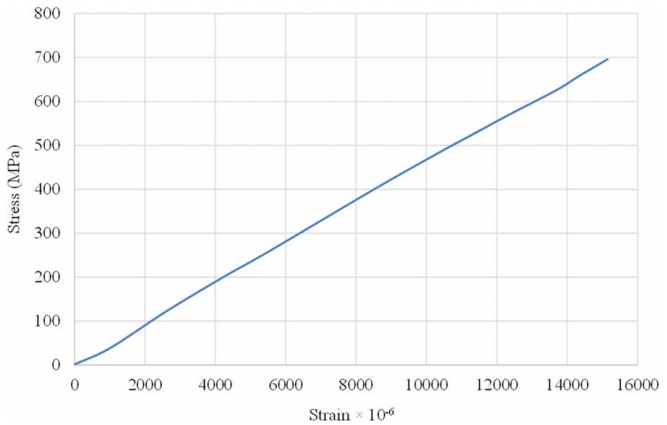

Fig. 13. Tensile stress–strain curve of flat coupon 2C taken from a 16-mm bar extracted from the Sierrita de la Cruz Creek Bridge.

between flat coupons and full-size bars, the strength of the current production full bars [823 MPa (119.3 ksi)] was divided by the strength of the current production flat coupons [670 MPa (97.2 ksi)], which resulted in a conversion rate of 1.23. The 23% difference in strength of the full bars versus flat coupons was attributed to factors that include fiber damage caused by the machining. Applying the 1.23 strength conversion ratio to the extracted flat

Table 7. Tensile test results for flat coupons from pristine current production 16-mm bars similar to those extracted from the Sierrita de la Cruz Creek Bridge (same manufacturer)

Specimen ID	Ultimate strength [MPa (ksi)]	Elastic modulus [GPa (ksi)]
1F	656 (95.2)	45.3 (6,575)
2F	635 (92.1)	—
3F	608 (88.1)	43.3 (6,287)
4F	709 (102.7)	44.5 (6,456)
5F	787 (114.1)	43.9 (6,363)
6F	618 (89.6)	45.8 (6,637)
7F	646 (93.7)	43.3 (6,287)
8F	675 (97.9)	44.8 (6,493)
9F	689 (99.9)	45.3 (6,577)
10F	678 (98.3)	43.3 (6,278)
Average	670 (97.2)	44.4 (6,439)
Std. deviation	52 (7.5)	1.0 (140)

Table 8. Tensile test results for pristine current production 16-mm bars similar to bars extracted from the Sierrita de la Cruz Creek Bridge (same manufacturer)

Specimen ID	Ultimate strength [MPa (ksi)]	Elastic modulus [GPa (ksi)]
1	830 (120.4)	49.7 (7,215)
2	845 (122.6)	51.7 (7,490)
3	792 (114.9)	51.6 (7,476)
4	829 (120.2)	50.8 (7,367)
5	849 (123.2)	51.4 (7,451)
6	784 (113.8)	51.6 (7,488)
7	834 (120.9)	—
8	828 (120.0)	50.4 (7,302)
9	813 (118.0)	52.5 (7,614)
10	822 (119.3)	52.8 (7,658)
Average	823 (119.3)	51.4 (7,451)
Std. deviation	21 (3.0)	1.0 (140)

Note: The nominal bar area used in the calculations was 200 mm^2 (0.31 $in.^2$).

Table 9. Tensile test results for pristine 16-mm bars identical to those in the Sierrita de la Cruz Creek Bridge tested in 2000

Specimen ID	Ultimate strength [MPa (ksi)]	Elastic modulus [GPa (ksi)][a]
1	801 (116.2)	—
2	843 (122.3)	—
3	735 (106.6)	—
4	760 (110.3)	—
Average	785 (113.8)	40.8 (5,920)
Std. deviation	48 (6.9)	—

Note: The nominal bar area used in the calculations was 200 mm^2 (0.31 $in.^2$).
[a]Data from Phelan et al. (2003).

coupons provided a 765 MPa (111 ksi) estimated strength for full extracted bars. The strength and modulus of the full bars manufactured and tested during 2000 were 785 MPa (113.8 ksi) and 40.8 GPa (5,920 ksi), as listed in Table 9. Therefore, the estimated strength reduction of the full bars extracted from the bridge after 17 years of service, found by comparing the 765 MPa (111 ksi) estimated extracted bar strength with the 785 MPa (113.8 ksi) published strength of bars used to construct the bridge, was 2.5%. It is noted that the elastic modulus of the extracted bars was approximately 20% higher than the original bars. This apparent increase over time was due to the unjustified low elastic modulus obtained in the 2000 test. First, only one value was provided and second, and most importantly, this value was significantly lower than the average value (48.6 GPa) obtained by the manufacturer in these years

Table 10. Bar constituent contents, in percent by volume, according to image analysis (mean ± std. deviation)

Specimen ID	Fiber volume content (%)	Matrix volume content (%)	Void volume content (%)
CO_C2B_B2	53.3 ± 6.6	46.1 ± 6.8	0.5 ± 0.8
CO_C3_B2	52.3 ± 5.3	47.0 ± 5.1	0.7 ± 0.6
CO_C5_B2	53.5 ± 9.6	45.9 ± 9.7	0.6 ± 0.9

during routine quality control tests (D. Gremel, personal communication, 2017).

If the degradation rate of the bars was hypothesized to be linear with time, tensile strength would be reduced by 15% over 100 years. However, based on the evidence that the creep rupture strength of GFRP varies with log-time rather than time itself (Greenwood 2002; Bakis et al. 2005), the 100-year strength reduction would be 3.6%. Therefore, it should be considered that the rate of change strength over time could be expected to vary, which depends on the sustained stress carried by the bars, the diameter of the bars, the materials used to manufacture the bars, and the local environmental details, such as temperature, chemical exposure, and condition of the concrete (Nkurunziza et al. 2002). For the Sierrita de la Cruz Creek Bridge, the bars were manufactured from of E-glass fiber and vinyl–ester resin and had a 15.9 mm concrete cover. In addition, the concrete near the bars had a high pH of 11.5, although carbonation was suspected to have reached the level of the bars (Benzecry et al., forthcoming).

Constituent Volume Contents by Image Analysis

Table 10 lists the fiber, matrix, and void volume contents of O'Fallon bars based on image analysis. The fiber volume contents were between 52.3% and 53.5% and the void volume contents were from 0.5% to 0.7%. Void contents <1% were generally considered to represent well-consolidated composites.

Conclusions and Recommendations

To help overcome barriers to the deployment of GFRP bars in the construction industry, an extensive investigation into the durability of GFRP reinforcement bars extracted from bridges built 15–20 years ago was undertaken. Several mechanical and physical tests were conducted on these bars. In addition to the bar tests, concrete tests were performed to evaluate the surrounding environment of the bars (Benzecry et al., forthcoming). Overall, the test results suggest that GFRP bars could be considered a promising replacement for steel reinforcement in bridge decks that are subjected to deicing salts. The following list summarizes the outcomes of the individual tests on the bars and provides recommendations for future investigations.

1. Fiber mass content: Burn-off tests on bars from all 11 bridges determined that the fiber mass content of the bars, which included filler particles allowed in ASTM D7957 (ASTM 2017a), met or exceeded the 70% requirement of ASTM D7957 (ASTM 2017a) with only one exception. The single exception was 69.2%. It is recommended that improved experimental procedures should be developed to account for residual filler stuck to the fibers.
2. Water absorption: Water uptake to equilibrium at 50°C (122°F), relative to a superficially dried initial condition, was <1% in bars from 5 of the 8 tested bridges and between 1.5% and 2.1% for the other 3 bridges. Some bars exceeded the contemporary 1% limit for bar qualification in ASTM D7957 (ASTM 2017a); it should be considered that these bars were manufactured before any bar material standards existed. In addition, it is recommended that methods to quantify moisture uptake should be developed to overcome difficulties caused by the water-induced loss of surface materials applied to the bars for bond enhancement, such as sand particles.
3. Moisture content: Based on dry-out tests, the moisture content in the as-received bars from two bridges was between 0.32% and 0.44%.The as-received moisture content of the bars was not expected to be saturated due to field exposure; however, the measured moisture contents were noted to be well below the 1% equilibrium value stipulated in ASTM D7957 (ASTM 2017a) as a limit for durable GFRP bars.
4. SEM: A minimal amount of microcracking was observed in the matrix and fibers of the bars from all 11 bridges. Some of the observed damage was attributed to specimen polishing and other damage was attributed to environmental degradation due to its concentration near the outer radius of the bars.
5. EDS: Zr was not observed in the fibers of bars from any of the 11 bridges, which indicated that the bars were not alkali-resistant. No chemical evidence of leaching of fiber material into the matrix was observed. In one bridge, Na found in the matrix of the bar was attributed to ingress from the environment, because it was not found in the fibers of the same bar. The availability of the EDS results on similar bars tested at the time of installation would have enabled more certain evaluations in the changes of atomic species over the service life.
6. T_g: Extracted bars from all bridges had T_g values between 80% and 115°C (239 F), with approximately half >80°C, the limit stipulated in ASTM D7957 and half below that limit. Data on T_g at the time of installation of the bars would be required to determine if the T_g decreased due to service conditions or if it was low from the outset due to resin choice or incomplete curing.
7. SBS: The SBS strength of bars extracted from 8 bridges was from 30 to 47 MPa (4,316 to 6,809 psi), which implied strength retention of 72%–92% in the 3 cases where identical bars were tested at the time of bridge construction. Bars at the weaker end of the spectrum were noted to be at the shorter end of the standardized span-to-diameter ratio limit.
8. Tensile test: Based on a special method developed to evaluate the strength of flat tensile coupons extracted from bars and relating the flat coupon strength to the strength of full-size bars, it was concluded that extracted bars from one bridge had a reduction in tensile strength of 2.5% after 17 years of service. Extrapolating this result to 100 years, the predicted tensile strength would be reduced by 15% if the extrapolation was linear in time and 3.6% if it was linear in log-time. In the future, additional tensile test data from extracted bars should be obtained to improve confidence in these conclusions.
9. Constituent volume contents by image analysis: Image analysis has certain advantages over burn-off testing, because it provides a measure of void volume content as well as fiber volume content uncontaminated by filler material. Bar specimens from one bridge had void volume contents between 0.5% and 0.7% and fiber volume contents between 52.3% and 53.5%.

Data Availability Statement

Some or all data, models, or codes that support the findings of this study are available from the corresponding author upon reasonable request.

Acknowledgments

The authors gratefully acknowledge support from the American Concrete Institute's Strategic Development Council the ReCAST Tier 1 University Transportation Center at the Missouri University of Science and Technology, The United States Department of Education GAANN Program, and NSF I/UCRC CICI (Grant # NSF-1916342). Deeply appreciated is the technical assistance from staff at Owens Corning (Mr. Ryan Koch and Mrs. Mala Nagarajan), University of Miami (Ms. Janna Brown and Mr. Jorge Alvarez), Missouri S&T (Dr. Clarissa Wisner and Mr. Eric Bohannan), and Pennsylvania State University (Mr. Jeffrey Kim and Mr. Jinhoo Kim. The opinions expressed in this material are those of the authors and do not necessarily reflect the views of sponsoring agencies.

References

ACI (American Concrete Institute). 2015. *Guide for the design and construction of structural concrete reinforced with fiber-reinforced polymer bars*. ACI 440.1R. Farmington Hills, MI: ACI.

Al-Salloum, Y. A., S. El-Gamal, T. H. Almusallam, S. H. Alsayed, and M. Aqel. 2013. "Effect of harsh environmental conditions on the tensile properties of GFRP bars." *Composites, Part B* 45 (1): 835–844. https://doi.org/10.1016/j.compositesb.2012.05.004.

ASTM. 2010. *Standard test method for moisture absorption properties and equilibrium conditioning of polymer matrix composite materials*. ASTM-D5229. West Conshohocken, PA: ASTM.

ASTM. 2011a. *Standard guide for identification of fiber-reinforced polymer-matrix composite materials in databases*. ASTM E1309. West Conshohocken, PA: ASTM.

ASTM. 2011b. *Standard test method for tensile properties of fiber reinforced polymer matrix*. ASTM-D7205. West Conshohocken, PA: ASTM.

ASTM. 2011c. *Test method for ignition loss of cured reinforced resins*. ASTM D2584-11. West Conshohocken, PA: ASTM International.

ASTM. 2013. *Standard test method for assignment of the glass transition temperature by dynamic mechanical analysis*. ASTM E1640-13. West Conshohocken, PA: ASTM International.

ASTM. 2014a. *Standard test method for assignment of the glass transition temperatures by differential scanning calorimetry*. ASTM-E1356. West Conshohocken, PA: ASTM.

ASTM. 2014b. *Standard test method for tensile properties of polymer matrix composite materials*. ASTM D3039/D3039M. West Conshohocken, PA: ASTM.

ASTM. 2016. *Standard test method for apparent horizontal shear strength of pultruded reinforced plastic rods by the short-beam method*. ASTM-D4475. West Conshohocken, PA: ASTM.

ASTM. 2017a. *Standard specification for solid round glass fiber reinforced polymer bars for concrete reinforcement*. ASTM-D7957. West Conshohocken, PA: ASTM.

ASTM. 2017b. *Standard test method for water absorption of plastics*. ASTM-D570. West Conshohocken, PA: ASTM.

Bakis, C. E., T. E. Boothby, R. A. Schaut, and C. G. Pantano. 2005. "Tensile strength of GFRP bars under sustained loading in concrete beams." *ACI Symp. Publ.* 230: 1429–1446.

Becker, H., and L. E. Locascio. 2002. "Polymer microfluidic devices." *Talanta* 56 (2): 267–287. https://doi.org/10.1016/S0039-9140(01)00594-X.

Benmokrane, B., C. Nazair, M. A. Loranger, and A. Manalo. 2018. "Field durability study of vinyl-ester-based GFRP rebars in concrete bridge barriers." *J. Bridge Eng.* 23 (12): 04018094. https://doi.org/10.1061/(ASCE)BE.1943-5592.0001315.

Benzecry, V., A. F. Al-Khafaji, R. T. Haluza, C. E. Bakis, J. J. Myers, and A. Nanni. Forthcoming. "Durability assessment of 15- to 20-year-old GFRP bars extracted from bridges in the US. II: Selected bridges, bar extraction, and concrete assessment." *ASCE J. Compos. Constr*. https://doi.org/10.1061/(ASCE)CC.1943-5614.0001110.

Chen, Y., J. Davalos, and I. Ray. 2006. "Durability prediction for GFRP reinforcing bars using short-term data of accelerated aging tests." *J Compos. Cons.* 10 (4): 279–286. https://doi.org/10.1061/(ASCE)1090-0268(2006)10:4(279).

Diamond, S. 1981. "Effects of two Danish flyashes on alkali contents of pore solutions of cement fly ash pastes." *Cem. Concr. Res.* 11 (3): 383–394. https://doi.org/10.1016/0008-8846(81)90110-1.

Ghiorse, S. R. 1991. *A comparison of void measurement methods for carbon/epoxy composites*. Watertown, MA: U.S. Army Materials Technology Laboratory.

Gooranorimi, O., and A. Nanni. 2017. "GFRP reinforcement in concrete after 15 years of service." *J. Compos. Constr.* 21 (5): 04017024. https://doi.org/10.1061/(ASCE)CC.1943-5614.0000806.

Gooranorimi, O., J. Myers, and A. Nanni. 2017. "GFRP reinforcements in box culvert bridge: A case study after two decades of service." In *Concrete pipe and Box culverts*, edited by J. Meyer and J. Beakley, 75–88. West Conshohocken, PA: ASTM.

Greenwood, M. 2002. "Creep-rupture testing to predict long-term performance, durability of fiber reinforced polymer (FRP) composites for construction." In *Proc., 2nd Int. Conf. Durability of Fiber Reinforced Polymer for Construction*, 29–31. Montreal, Québec: Np.

Kamal, A. S. M., and M. Boulfiza. 2011. "Durability of GFRP rebars in simulated concrete solutions under accelerated aging conditions." *J. Compos. Constr.* 15 (4): 473–481. https://doi.org/10.1061/(ASCE)CC.1943-5614.0000168.

Khatibmasjedi, M., S. Ramanathan, P. Suraneni, and A. Nanni. 2020. "Durability of commercially available GFRP reinforcement in seawater-mixed concrete under accelerated aging conditions." *J. Compos. Constr.* 24 (4): 04020026. https://doi.org/10.1061/(ASCE)CC.1943-5614.0001035.

Koch, G., J. Varney, N. Thopson, O. Moghissi, M. Gould, and J. Payer. 2016. *International measures of prevention, application, and economics of corrosion technologies study*. Houston: NACE International.

Little, J. E., X. A. Yuan, and M. I. Jones. 2012. "Characterisation of voids in fibre reinforced composite materials." *NDT E Int.* 46 (Mar.): 122–127. https://doi.org/10.1016/j.ndteint.2011.11.011.

Micelli, F., and A. Nanni. 2004. "Durability of FRP rods for concrete structures." *Constr. Build. Mater.* 18 (7): 491–503. https://doi.org/10.1016/j.conbuildmat.2004.04.012.

Mufti, A., M. Onofrei, B. Benmokrane, N. Banthia, M. Boulfiza, J. Newhook, B. Bakht, G. Tadros, and P. Brett. 2007. "Durability of GFRP reinforced concrete in field structures." In *Proc., 7th Int. Symp. on Fiber Reinforced Polymer Reinforcement for Concrete Structures*, 6–9. Kansas City, MO: Np.

Murphy, K., S. Zhang, and V. M. Karbhari. 1999. "Effect of concrete based alkaline solutions on short term response of composites." In *Proc., 44th SAMPE Symp. and Exhibition*, edited by L. J. Cohen, J. L. Bauer, and W. E. Davis, 2222–2230. Long Beach, CA: Society for the Advancement of Material and Process Engineering.

Nanni, A., A. De Luca, and H. Zadeh. 2014. *Reinforced concrete with FRP bars*. London: CRC Press.

Nkurunziza, G., A. Debaiky, P. Cousin, and B. Benmokrane. 2005. "Durability of GFRP bars: A critical review of the literature." *Prog. Struct. Mater. Eng.* 7 (4): 194–209. https://doi.org/10.1002/pse.205.

Nkurunziza, G., R. Masmoudi, and B. Benmokrane. 2002. "Effect of sustained tensile stress and temperature on residual strength of GFRP composites." In *Proc., 2nd Int. Conf. Durability of Fiber Reinforced Polymer for Construction*, 347–358. Montreal, Quebec: Np.

Owens Corning. 2020. "Fiberglas dowel bars for load transfer between concrete slabs: Glass fiber reinforced polymer (GFRP) dowel bars." Product data sheet. Toledo, OH: Owens Corning. https://dcpd6wotaa0mb.cloudfront.net/mdms/dms/CSB/10022293/10022293-Owens-Corning®-Fiberglas™-Dowel-Bars-Data-Sheet-(3).pdf?v=1605111345000.

Phelan, R., W. Vann, and J. Bice. 2003. *FRP reinforcement bars in bridge decks: Field instrumentation and short-term monitoring*. Research Report: 9-1520-04. Lubbkock, TX: Texas Department of Transportation.

Porter, M. L., and B. A. Barnes. 1998. "Accelerated aging degradation of glass fiber composites." *In Second international conference on composites in infrastructure*, edited by H. Saadatmanesh and M. R. Eshani, 446–459. Tucson, AZ: University of Arizona.

Saadatmanesh, H., and F. E. Tannous. 1999. "Relaxation, creep, and fatigue behavior of carbon fiber-reinforced plastic tendons." *ACI Mater. J.* 96 (2): 143–153.

Sheridan, R. J., et al. 2017. "Road mapping workshop report on overcoming barriers to adoption of composites in sustainable infrastructure." *NIST Special Publication 1218*. https://doi.org/10.6028/NIST.SP.1218.

Taylor, H. 1987. "A method for predicting alkali ion concentration in cement pore water solutions." *Adv. Cem. Res.* 1 (1): 5–17. https://doi.org/10.1680/adcr.1987.1.1.5.

Trejo, D., P. Gardoni, and J. J. Kim. 2011. "Long-term performance of glass fiber-reinforced polymer reinforcement embedded in concrete." *ACI Mater. J.* 108 (6): 605–613.

Wang, Z., X. Zhao, G. Xian, G. Wu, R. K. S. Raman, and S. Al-Saadi. 2017. "Long-term durability of basalt- and glass-fibre reinforced polymer (BFRP/GFRP) bars in seawater and sea sand concrete environment." *Constr. Build. Mater.* 139 (May): 467–489. https://doi.org/10.1016/j.conbuildmat.2017.02.038.

Yang, W.-R., X.-J. He, L. Dai, L. Zhao, and F. Shen. 2016. "Fracture performance of GFRP bars embedded in concrete beams with cracks in an alkaline environment." *J. Compos. Constr* 20 (6): 04016040. https://doi.org/10.1061/(ASCE)CC.1943-5614.0000688.